striatal projection neuron. Therefore, the field of influence of any particular efferent neuron at its target nuclei, as defined by the position and the extent of its terminal arborizations, must take synaptic contacts on long dendrites into consideration. Neurons with cell bodies outside of an apparent afferent terminal field still could be directly influenced by that afferent source.

Our results also show that even though all of the identified neostriatal efferent neurons are medium spiny neurons, the distribution of their main axons could be very different. This demonstrates that neurons with similar somato-dendritic morphology that receive similar afferent inputs can have different projection patterns and thus differ considerably in function.

H. T. CHANG
C. J. WILSON, S. T. KITAI
Department of Anatomy, Michigan State University, East Lansing 48824

References and Notes

1. P. J. Snow, P. K. Rose, A. G. Brown, *Science* **191**, 312 (1976); S. Cullheim and J. O. Kellerth, *Neurosci. Lett.* **2**, 307 (1976); E. Jankowska, J. Rastad, J. Westman, *Brain Res.* **105**, 557 (1976).
2. S. T. Kitai, J. D. Kocsis, R. J. Preston, M. Sugimori, *Brain Res.* **109**, 601 (1976).
3. J. M. Kemp and T. P. S. Powell, *Philos. Trans. R. Soc. London Ser. B* **262**, 383 (1971); C. A. Fox, A. N. Andrade, D. E. Hillman, R. C. Schwyn, *J. Hirnforsch.* **13**, 181 (1971–1972); M. DiFiglia, P. Pasik, T. Pasik, *Brain Res.* **114**, 245 (1976).
4. R. J. Preston, G. A. Bishop, S. T. Kitai, *Brain Res.* **183**, 253 (1980).
5. C. J. Wilson and P. M. Groves, *J. Comp. Neurol.* **194**, 599 (1980); G. A. Bishop. H. T. Chang, S. T. Kitai, *Soc. Neurosci. Abstr.* **5**, 67 (1979); H. T. Chang, G. A. Bishop, S. T. Kitai, *ibid.*, p 69.
6. Intracellularly recorded striatal neurons were labeled with HRP by passage of 2 to 5 nA (300 msec duration, 50 percent duty cycle) of positive ejection pulses through recording electrodes filled with 4 percent HRP in 0.05*M* tris-HCl buffer (*p*H 7.6) and 0.5*M* potassium chloride or potassium methylsulfate. Rat brains were fixed by intracardial perfusion of buffered Ringer solution followed by a solution of 2 percent formaldehyde and 2 percent glutaraldehyde in 0.15*M* phosphate buffer (*p*H 7.4). Survival periods following intracellular labeling ranged from 2 to 6 hours. Serial vibratome sections were cut in the sagittal plane and processed for light and electron microscopic analysis as described by C. J. Wilson and P. M. Groves [*J. Neurosci. Methods* **1**, 383 (1979)]. With frequent light microscopic examination of the block face during thin sectioning, individual axons and boutons were identified by both light and electron microscopy.
7. P. Somogyi and A. D. Smith, *Brain Res.* **178**, 3 (1979).
8. I. Grofova, in *The Neostriatum*, I. Divac and R. G. E. Oberg, Eds. (Pergamon, Oxford, 1979), pp. 37–52.
9. J. M. Kemp, *Brain Res.* **17**, 125 (1970); I. Grofova and E. Rinvik, *Exp. Brain Res.* **11**, 249 (1970).
10. C. A. Fox, J. A. Rafols, W. M. Cowan, *J. Comp. Neurol.* **159**, 201 (1975).
11. C. A. Fox and J. A. Rafols, *ibid.*, p. 177.
12. Unpublished observations (W. Falls, M. R. Park, S. T. Kitai) on both intracellularly labeled GP neurons and Golgi impregnated material indicate that most GP neurons in the rat have dendrites extending up to 1 mm away from the soma.
13. We thank B. Bitzinger and C. Meister for their skillful assistance in photograph and manuscript preparations. This study was supported by Public Health Service grant NS 14866 to S.T.K. and NS 17294 to C.J.W.

16 December 1980; revised 17 February 1981

Electrical Potentials in Human Brain During Cognition: New Method Reveals Dynamic Patterns of Correlation

Abstract. *A new technique has been developed for identifying, in humans, dynamic spatiotemporal electrical patterns of the brain during purposive behaviors. In this method, single-trial time-series correlations between brain macropotentials recorded from different scalp sites are analyzed by distribution-independent mathematical pattern recognition. Dynamic patterns of correlation clearly distinguished two brief visuomotor tasks differing only in type of mental judgment required (spatial or numeric). These complex patterns shifted in the anterior-posterior and left-right axes between successive 175-millisecond intervals, indicating that many areas in both cerebral hemispheres were involved even in these simple judgments. These patterns were not obtainable by conventional analysis of averaged evoked potentials or by linear analysis of correlations, suggesting that the new technique will advance the study of human brain activity related to cognition and goal-directed behaviors.*

The use of correlation measures of brain macropotentials, recorded as electroencephalogram (EEG) time series, for studying mass neural processes related to purposive behaviors (*1–3*) is based on the hypothesis that during purposive behaviors in humans many cortical and subcortical areas are functionally related (*4*). Although the means of communication between these areas and the relation of such communication to macropotentials are not well understood (*5*), there is evidence that increasing functional interrelation between neural areas may be reflected in increased correlation of their low-frequency macropotentials, independent of voltage (*6*).

Here we report the existence of macropotential correlations in humans related to type of mental judgment. Two visuomotor tasks requiring two types of cognitive judgment were performed while a high degree of control over stimulus-, response-, and performance-related factors was maintained. Small differences in patterns of correlation between tasks were extracted by applying distribution-independent mathematical pattern recognition, without signal averaging which obscures the individual-trial interareal phase relations. The results show spatially and temporally differentiated patterns of correlation delineating both the time course of mass neural processes associated with each task and the essential differences between tasks.

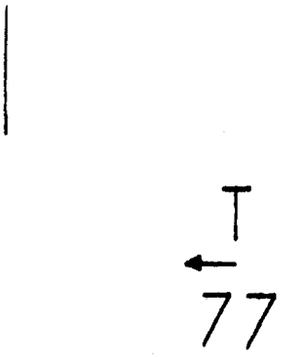

Fig. 1. Typical stimulus for arrow and number tasks. The stimulus subtended less than 2° visual angle. The participant was instructed either to produce a force which would cause the target (vertical line at left) to intersect the arrow's projection or to produce a force corresponding to the magnitude of the number, by a graded isometric contraction of the index finger. Differences in accuracy and response time were equalized between tasks by on-line computer adjustment of difficulty. Thus the two different cognitive tasks had the same stimuli, were performed equally well, and had the same response. Average response time was 1.2 seconds.

The challenging, brief (about 1.2 seconds) visuomotor task presumably established functional relations between visual, parietal, motor, frontal, and other neural areas. After a task cue was presented, a simple visual stimulus (an arrow, a target, and a number) was presented (Fig. 1) requiring a judgment of magnitude. The response was to exert a force on an isometric transducer with a ballistic contraction of the right index finger, proportional either to the distance the target would have to move to intersect the arrow's projection, or to the magnitude of the number (on a scale of 1 to 100). Arrow and number stimuli were always presented together, and the participant was task-cued in randomly ordered blocks of 13 trials (*7*). Performance-related factors were equalized between tasks by computer-controlled, on-line adjustment of the target size (arrow task) and the accuracy tolerance (number task) (*8*).

Five clinically normal, right-handed adults (four males, one female) each performed a total of about 270 trials. Sixteen electrodes were placed according to standard skull landmarks in positions covering the cranium (*9*). Vertical and horizontal eye movements, flexor muscle activity of the right index finger, and the resultant output of the isometric force transducer were recorded.

For each person, sets of trials of each

0036-8075/81/0821-0918$01.00/0

task were selected so that there were no significant between-task differences in stimulus-, response-, and performance-related factors (*10*). Stimulus-registered and response-registered averaged evoked potentials were then computed for each person and examined for consistent changes across tasks in peak latency or amplitude of the N1 (N170), P2 (P240), P3a (P340), P3b (P450), P4 (P620), and RP (readiness potential) components (Fig. 2). No task-related amplitude or latency shifts were consistent across persons, except for the P340 component, which was always larger for the number task at midline, left, and right parietal electrodes (*11*).

Since a component of the averaged evoked potential signifies the occurrence of neural processes which are consistently related in time to the stimulus, time intervals of 175 or 300 msec were centered on the peak time of the N1-P2, P3a, P3b, and P4 components of each person's averaged evoked potentials. Single-trial cross-correlation functions were computed between 44 pairwise combinations of 15 electrodes for each of these four latency intervals, as well as a 300-msec prestimulus and a 175-msec preresponse interval (*12*). The zero-lag correlation for each channel pair ranged from .98 for the midline frontal to midline premotor pair, to .38 for the midline frontal to midline occipital and right frontal to midline parietal pairs. Mean correlation values for each latency interval were: prestimulus = .74, N1-P2 = .81, P3a = .79, P3b = .75, P4 = .75, preresponse = .76. The trend for the prestimulus correlation to be lower than the N1-P2 or P3a correlations is consistent with the idea that increasing correlations accompany stimulus-related neural processing. The only significant task-related effect revealed by an analysis of variance was a task times channel-pair interaction in the N1-P2, P3a, and P3b intervals (*13*). To elucidate spatial patterns, we performed a separate analysis by standardizing (mean = 0, standard deviation = 1) all single-trial correlations within each person's data between the number and arrow tasks and performing a *t*-test for each of the 44 correlations in each of the six intervals. Only four correlations were significantly different ($P < .05$, Bonferroni corrected for multiple comparisons) between tasks: right frontal–midline frontal, left frontal–midline precentral in the N1-P2 interval; midline occipital–midline parietal, and midline occipital–midline posterior parietal in the P4 interval.

Since these linear statistical methods were not informative, nonlinear, distribution-independent, multivariate pattern recognition was applied to determine how the correlation patterns of each task changed with time and whether the two tasks had contrasting correlation patterns within each latency interval (*14, 15*). For the within-task analysis, Fisher Z'-transformed correlations were converted to standard scores between latency intervals for each person and electrode pair. For the between-task analysis, the correlations were standardized between tasks for each person, latency interval, and electrode pair. The 44 pairwise combinations of the 15 electrodes were grouped into nine major cortical areas in overlapping fashion: right or left frontal, central, and parietal electrodes were each combined with their midline electrodes; right or left temporal and parietal were grouped together; occipital recording was only midline. The pattern recognition algorithm then computed mathematical classification functions to distinguish the change between time intervals for each task, or to distinguish the arrow and number tasks within each interval. Functions were derived for each of the nine areas, and consisted of a nonlinear polynomial of the correlations of the particular area usually with 10 or 11 other areas. Each classification function was developed on 788 trials, and cross-validation was achieved by presenting 400 previously unanalyzed trials to each classification function. The correlations of a particular area were deemed to have changed with time or to have differed between tasks if the cross-validation classification accuracy was significant at $P < .005$ or better. [Forty-nine attempted classifications with the data randomly assigned to the arrow or number categories did not produce significant cross-validation classifications at $P < .005$ (*16*).] For each significant classification, correlations contributing most prominently were evaluated from the classification function by a previously developed algorithm (*17*). Finally, the significant areas and signs of prominent correlations contributing to the significant classifications were formed into diagrams.

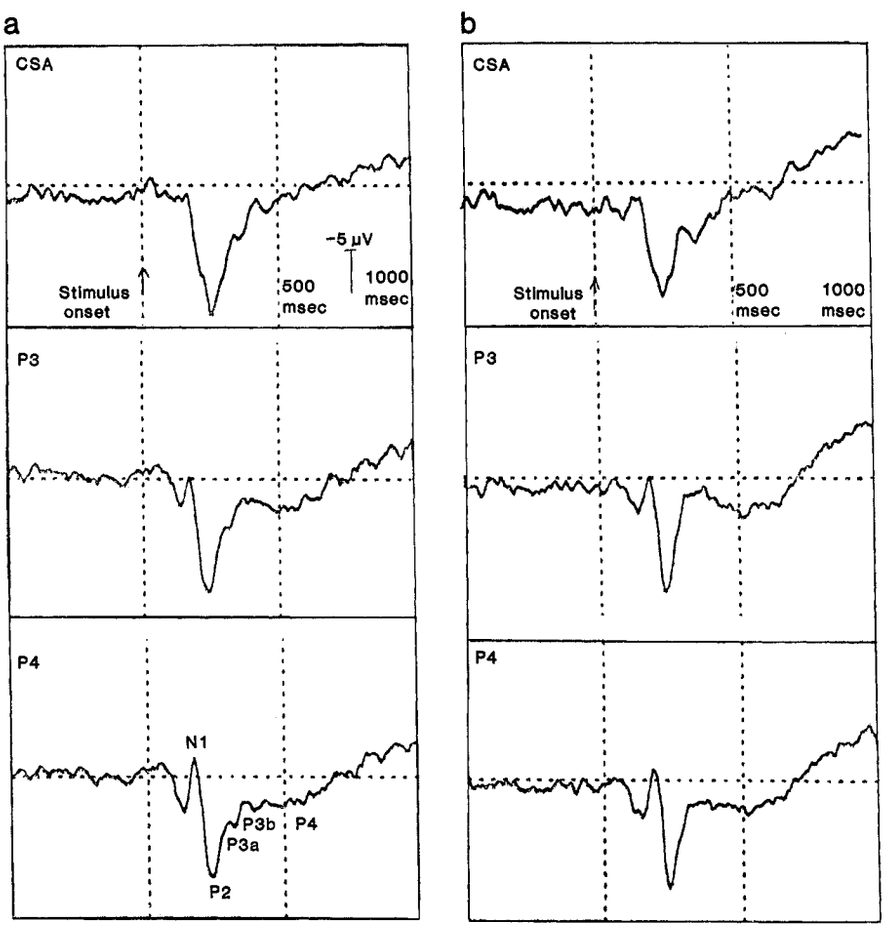

Fig. 2. Composites (average of averages) of five participants' stimulus-registered averaged evoked potentials for (a) number and (b) arrow tasks. Each composite is made up of about 55 trials from each of the five participants [277 trials in (a), 279 trials in (b)]. There were no consistent differences between tasks in the peak amplitudes or latencies of the individual averages forming the composite, except for the P3a (P340) component, which had a slightly larger amplitude parietally in the number task.

The diagrams of the within-task analysis reveal similarities between tasks in the anatomic distribution of changes in correlation between intervals (Fig. 3, a and b). The changes were greater in the number task from the prestimulus to the P3a interval and in the arrow task from the P3a to the P4 interval. From the prestimulus to the N1-P2 interval almost all areas changed, with most correlations increasing. From the N1-P2 to the P3a interval, left temporo-parietal and midline-right central areas changed in the arrow task; bilateral temporo-parietal, midline-left central, midline-left parietal, and midline-bilateral frontal areas changed in the number task. From the P3a to the P3b interval, bilateral temporo-parietal, midline-bilateral parietal, and midline occipital areas changed in the arrow task; right temporo-parietal, midline-right central, and midline-left frontal areas changed in the number task. Most posterior correlations decreased in both tasks. From the P3b to the P4 interval, the areas showing change were identical for both tasks: midline-bilateral frontal and central. Frontal to midline precentral correlations decreased, whereas midline precentral to left parietal increased in both tasks. From the P4 to the preresponse interval, changes in midline-bilateral areas predominated in the arrow task, whereas all areas changed in the number task. The involvement of the midline precentral area in many of these interval changes may be associated with the preparation of deliberate motor acts, a finding which is consistent with recent radiologic data (*18*).

The pattern recognition analysis was then applied to determine how the arrow and number tasks differed from each other in each latency interval (*19*). Significant differences were found in all but the preresponse interval (Fig. 3c). In the prestimulus interval significant differ-

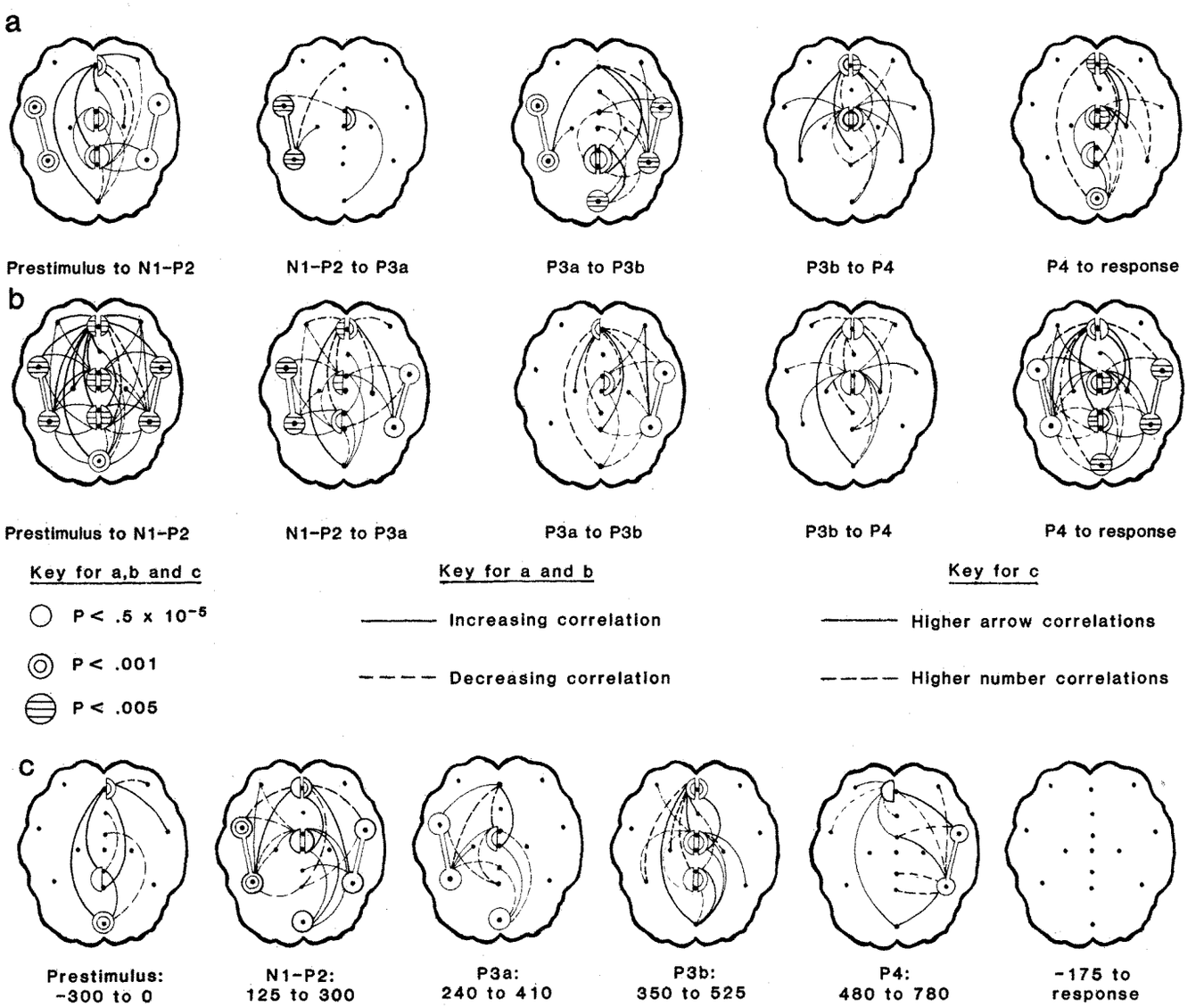

Fig. 3. (a) Within-task pattern recognition analysis for the arrow task; areas outlined are those whose unaveraged time-series correlations with other areas changed significantly from interval to interval; shading indicates the significance level of change. Prominent correlations are indicated by connecting lines: a correlation increasing with time is indicated by a solid line and decreasing correlation by a broken line. (b) Within-task pattern recognition analysis for the number task. Note the similarities with the arrow task (a) in the prestimulus to N1-P2 changes and P3b to P4 changes, as well as the differences in the N1-P2 to P3a and P3a to P3b changes. (c) Between-task pattern recognition analysis for each interval; areas outlined differed significantly in their correlation with other areas: a solid line connecting two areas indicates that the areas were more highly correlated for the arrow task, while a broken line indicates a higher correlation for the number task. Note the contrasts between the arrow and number tasks in the prestimulus interval, a finding which might be interpreted as evidence of a "preparatory set." Also, the lack of contrast in the preresponse interval may be interpreted as the completion of task-specific perceptual processing.

ences occurred in midline-right frontal, midline-left parietal, and midline occipital areas. Higher frontal-posterior correlations were found in the arrow task. In the N1-P2 interval, contrasts were seen in all areas except midline-left and midline-right parietal. The between-task differences in correlation included a complex picture of lateralization: in the arrow task higher correlation of right parietal with midline sites, lower correlation of right temporal with midline sites, and lower correlations of left temporo-parietal areas with most midline sites. In the P3a interval, left temporo-parietal, midline-left central, and midline occipital areas differed. A left-sided lateralization of differences was evident, although the signs of correlation differences were mixed. During the P3b interval midline and bilateral frontal, central, and parietal areas showed contrast between tasks. Correlations were lower in the arrow task between left parietal and midline frontal and precentral sites. In the P4 interval, the correlations of the midline-left frontal, and of the right temporo-parietal with other areas differed. No contrast was seen in the preresponse interval.

These between-task contrasts could be attributed to "preparatory set," type of mental judgment, and task-specific preparation for response, since there were no differences in stimuli, in magnitude, duration, velocity, and acceleration of responses, in accuracy and response time, or in measures of "arousal," eye movements, or other types of artifact (*20*). The presence of frontal, parietal, and occipital contrasts during the cued prestimulus interval may be a sign of task-specific "preparatory set." The lack of contrast between tasks in the 175-msec preresponse interval suggests that task-specific perceptual processing was completed by this time, when motor control commands common to both tasks were presumably being generated.

Since a change in correlation pattern implies a change in activity of the underlying neural areas, these findings indicate that many areas in both hemispheres are involved in a complex manner even in simple judgments. As noted, few between-task differences were evident in a visual analysis of the amplitude and latency of the major components of the averaged evoked potential or in linear analyses of averaged or single-trial correlations.

Additional speculation about the significance of these correlation patterns must be deferred until this method has been applied more extensively and evaluated in the light of known neuroradiologic, neurophysiologic, and neuropsychologic findings. Once the method has been further validated, a better temporal and anatomic resolution of mass brain potential patterns associated with cognition and purposive behaviors may be available for both basic and clinical research.

ALAN S. GEVINS
JOSEPH C. DOYLE
BRIAN A. CUTILLO
ROBERT E. SCHAFFER
ROBERT S. TANNEHILL
JESS H. GHANNAM
VIRGINIA A. GILCREASE
CHARLES L. YEAGER

EEG Systems Laboratory and *Langley Porter Institute, University of California School of Medicine, San Francisco 94143*

References and Notes

1. Human spatial correlation patterns have been examined by W. Walter and H. Shipton, *Electroenceph. Clin. Neurophysiol.* **3**, 281 (1951); M. Livanov and associates (*2*); J. Busk and G. Galbraith, *Electroencephalogr. Clin. Neurophysiol.* **38**, 415 (1975); E. Callaway and P. Harris, *Science* **183**, 873 (1974). These investigators did not achieve an adequate degree of control of stimulus-, response-, and performance-related and cognitive aspects of tasks, or of electrical [see A. Gevins *et al.* (*3*)] contaminants due to eye and hand movements.
2. See summary in M. Livanov, *Spatial Organization of Cerebral Processes* [Halsted (Wiley), New York, 1977].
3. A. S. Gevins, G. M. Zeitlin, J. C. Doyle, C. D. Yingling, R. E. Schaffer, E. Callaway, C. L. Yeager, *Science* **203**, 665 (1979); A. S. Gevins, J. C. Doyle, R. E. Schaffer, E. Callaway, C. Yeager, *ibid.* **207**, 1006 (1980); A. Gevins and R. Schaffer, *CRC Crit. Rev. Bioeng.* **1980**, 1165 (1980); A. Gevins, *IEEE Trans. Patt. Anal. Machine Intell.* **2**, 383 (1980).
4. L. Deeke, B. Grozinger, H. Kornhuber, *Biol. Cybern.* **23**, 99 (1976); E. Evarts and C. Fromm, *Neurosci. Lett.* **5**, 267 (1977); R. Haaxma and G. Kuypers, *Brain* **98**, 239 (1975); E. Jones, J. Coulter, S. Hendry, *J. Comp. Neurol.* **181**, 291 (1978); D. Robinson, M. Goldberg, G. Stanton, *J. Neurophysiol.* **41**, 910 (1978); J. Lynch, V. Mountcastle, W. Talbot, T. Yin, *ibid.* **40**, 362, (1977); J. Stein, in *Cerebral Motor Control in Man: Long Loop Mechanisms*, J. Desmedt, Ed. (Karger, Basel, 1978), p. 107; W. Thach, in *ibid.*, p. 94.
5. The association of macropotentials with neural information processing has been demonstrated in the simpler case of the paleocortex by W. Freeman, *Mass Action in the Nervous System* (Academic Press, New York, 1975); *Biol. Cybernet.* **33**, 237 (1979); *ibid.* **35**, 21 and 221 (1979).
6. Studies in animals specifically reporting increased correlation of low-frequency macropotentials during goal-directed tasks include T. Efremova and V. Trush, *Acta Neurobiol. Exp.* **33**, 743 (1973); V. Dumenko, in *Electrophysiology of the Nervous System*, V. Rusinov, Ed. (Plenum, New York, 1970); see also M. Livanov (*2*).
7. The task cue was presented for 2.5 seconds and was followed immediately by the task stimulus. One and one-half seconds after completion of the participant's movement (mean response time, 1.2 seconds; average standard deviation within person, $\sigma = 0.3$; average standard deviation between persons, $\sigma = 0.15$), the screen displayed the participant's response as well as the correct response. One second later the screen was erased; another 1.8 seconds later the task cue for the next trial was presented. The task type was changed randomly in 34 blocks of 10 to 13 trials.
8. C. Kelley, *Hum. Factors* **11**, 43 (1969). Mean error and response time displayed no significant task-associated difference.
9. The placements of the electrodes were: Oz, "Oy," P3, P4, Pz, "Ps," C3, C4, Cz, "Cs," "CSA," F7, F8, Fz, T3, and T4, with linked mastoid reference. Electrodes in quotes indicate nonstandard placements intended to overlie areas of particular interest such as anterior occipital (Oy), anterior parietal (Ps), midline precentral (superior edge—Cs), and midline premotor (Csa) areas. The low-pass filter rolled off 40 dB/octave above 50 Hz, whereas the high-pass filter rolled off 6 dB/octave below 0.16 Hz. The sampling rate was 128 Hz. A digital filter was applied to eliminate frequency components above 12 Hz.
10. For each participant *t*-tests were computed between tasks for 15 stimulus-, response-, and performance-related variables including target size, move required, magnitude, peak velocity, and acceleration of move performed and resultant error and response time. For any unbalanced variables, trials at the extreme of the distribution were deleted until there were no significant ($P < .05$) differences.
11. A task-by-electrode-by-participants analysis of variance confirmed a task main effect [$F(1, 4) = 37.7$], but no task-by-electrode interaction. Correlated *t*-tests for the P3, P4, and Pz data were all significant at $P < .05$.
12. We used 175-msec intervals for N1-P2, P3a, and P3b. This was the briefest interval with stable correlations for calibration signals sampled at 128 Hz. We used 300 msec for the multipeaked P4 component interval. Because of limited computer memory, a representative subset of 44 of the 105 total combinations of 15 channels was chosen. Only the zero-lag correlation results are discussed here.
13. For each interval, each participant's data were converted into 44 mean Fisher Z'-transformed correlations for the arrow and the number tasks separately. These data were used to perform a task × channel-pair × participant analysis of variance, which revealed no task main effect, but significant task × channel-pair interactions in the N1P2, P3a, and P3b latencies [$F(43, 172) = 3.55$, 1.76, 1.96, respectively, each $P < .01$]. There was a significant channel-pair effect in all latencies [$F(43, 172) = 47.5$ to 97.2, $P < .0001$].
14. A. Gevins, G. Zeitlin, C. Yingling, J. Doyle, M. Dedon, R. Schaffer, J. Roumasset, C. Yeager, *Electroencephalogr. Clin. Neurophysiol.* **47**, 693 (1979).
15. S. S. Viglione, in *Adaptive Learning and Pattern Recognition Systems*, J. Mendel and K. Fu, Eds. (Academic Press, New York, 1970), pp. 115–161).
16. Pattern recognition analyses were optimized to facilitate an anatomic interpretation of results, rather than to attain the highest level of classification accuracy; $P < .005$ corresponded to approximately > 56.5 percent correct cross-validation classification, $P < .001$ was > 58 percent, and $P < 5 \times 10^{-5}$ was > 60.0 percent, based on the binomial test. The pattern recognition results were examined for each participant separately for representative significant classifications in each of four latency intervals, and the ratio of his or her percentage performance to the cumulative percentage performance was averaged over the four classifications. The range of these average ratios over participants was 0.97 to 1.05, indicating consistency among participants.
17. See A. Gevins *et al.* (*14*). A classification function consisted of a linear combination of the binary (for example, arrow task or number task) decisions of one to seven discriminant functions. Each discriminant function consisted of a linear combination of six correlations. To select prominent correlations for display, we retained each combination of correlations (discriminant function) whose weight was more than 0.1 times the maximum weight given to any combination. Within the selected combinations, those correlations were chosen whose weight was more than 0.5 times the maximum weight of any correlation comprising the combination. This procedure was previously validated by determining that significant classification accuracy could still be obtained by using only the prominent features.
18. Activation of the "supplementary motor" area during voluntary movement in humans suggested it is a "supramotor" control area [J. M. Orgogozo and B. Larsen, *Science* **206**, 847 (1979)].
19. Behavioral deficits of patients with brain lesions imply greater involvement of right and left parietal areas, respectively, in performing tasks similar to the arrow and the number tasks [A. Benton, in *Clinical Neuropsychology*, K. Heil-

man and E. Valenstein, Eds. (Oxford Univ. Press, New York, 1979); A. Benton, H. Levin, N. Varney, *Neurology* **25**, 907 (1975)].
20. Possible between-task differences in saccadic scanning raises the qustion of artifactual origin of the results. Several considerations counterindicate this: (i) Trials with eye movements visible in the electrooculogram (EOG) were eliminated; averaged EOG's from trials used revealed no consistent differences between the tasks. (ii) Contamination due to potentials generated by eye movements should be strongest in the frontal regions, whereas the patterns extracted by pattern recognition were varied and included the whole scalp. Frontal differentiation was not the most accurate (parietal differentiation during the P3b interval was most accurate), and it was not significant during the N1-P2 interval, which is just after the minimum time required to produce a saccade. And (iii) the presence of spatially differentiated patterns during the cued prestimulus interval and the lack of differences just prior to response support the interpretation of neural genesis of the results.
21. Supported in part by grants from the Public Health Service, the Office of Naval Research, the Fetzer Foundation, and Marilyn Brachman-Hoffman. We thank S. Bressler, E. Callaway, W. Davis, W. Freeman, B. Garoutte, E. Halgren, D. Jewett, B. Libet, A. Salamy, C. Skomer, and S. Viglione for critically reviewing the first seven drafts of the manuscript, H. Currens for manuscript preparation, and S. Bowman for the artwork.

8 April 1981; revised 22 June 1981

DDT-Induced Feminization of Gull Embryos

Abstract. *Injection of DDT [1,1,1-trichloro-2,2-bis(p-chlorophenyl)ethane] into gull eggs at concentrations comparable to those found in contaminated seabird eggs in 1970 induces abnormal development of ovarian tissue and oviducts in male embryos. Developmental feminization of males is associated with inability to breed as adults and may explain the highly skewed sex ratio and reduced number of male gulls breeding on Santa Barbara Island in southern California.*

Between 1950 and 1970 offshore southern California was subjected to massive contamination by the discharge of as much as 1.9 million kilograms of commercial DDT (*1*) from the Los Angeles sewer system (*2*, *3*). This resulted in high residues of total DDT (*4*) at all levels of the ecosystem, with particularly high concentrations in fish, sea lions, and seabirds (*5*). The breeding failure of brown pelicans (*Pelecanus occidentalis*) and double-crested cormorants (*Phalacrocorax auritus*) due to eggshell thinning has been well documented (*6*–*8*). High concentrations were measured in eggs of western gulls (*Larus occidentalis*) 3 years after sewer discharge of DDT ceased (*9*).

We report that DDT contamination of eggs during the early 1970's may be involved in the current reproductive failure of western gulls in the Channel Islands. The poor breeding success is characterized by a reduced number of adult males, a highly skewed sex ratio (3.85 females for each male on Santa Barbara Island), and female-female pairing of some of the excess females (*10*). We propose that DDT contamination of eggs and embryos causes abnormal development of the reproductive system and results in breeding failure in the adult birds.

Gull eggs are relatively insensitive to the thinning effects of DDT (*11*). Concentrations that result in severely thinned and broken pelican eggs (40 to 80 ppm per whole egg, by weight) (*12*) result in only modest (6 to 10 percent) thinning in gull eggshells; embryos survive until concentrations reach 200 to 300 ppm (*13*). However, this resistance to eggshell thinning puts gull embryos at greater risk of exposure to the estrogenic effects of DDT metabolites. We exposed gull embryos to DDT at historical levels (2 to 100 ppm) to determine the effects that probably occurred in the wild.

Eggs were collected in 1979 and 1980 from breeding colonies at Mono Lake (California gulls, *Larus californicus*) and Southeast Farallon Island (western gulls). These places do not have a history of high DDT contamination. An attempt was made to obtain unincubated eggs by collecting the first egg laid in a nest at the beginning of the nesting season. Recrystallized pesticides and metabolites or estradiol were dissolved in corn oil and injected directly into the yolk (*14*). This method closely approximates the distribution of the pollutants in eggs in the wild, since these compounds are lipid-soluble and accumulate in yolk. The injected pollutants do not immediately mix with yolk, but become mixed as the yolk is mobilized during the first few days of incubation. Injected eggs were incubated artificially (*15*), and embryos that survived to hatching were fixed and examined.

Two hundred sixty-four eggs were successfully injected, and 108 developed to pipping, the point at which the embryo is ready to cut the shell with its egg tooth. Many embryos died (45 percent died before they had been incubated for 2 days), probably because of transport, storage, and injection. Data from both species were pooled since no differences were observed in sensitivity to the compounds or extent of developmental abnormalities.

The anatomy of gulls at hatching and their response to estradiol or estrogenic compounds resemble those of chickens and Japanese quail (*16*, *17*), but gulls are much more sensitive to the effects of estrogens. All male embryos at all doses of estradiol were feminized. The extent

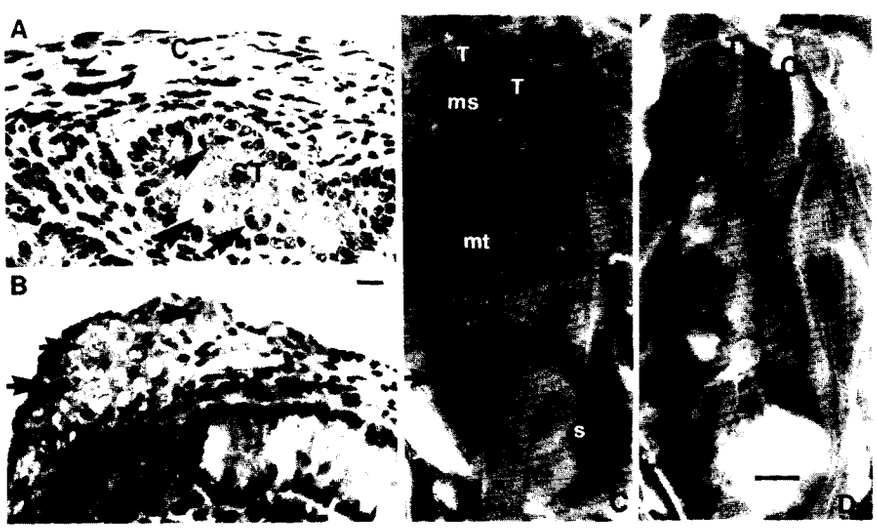

Fig. 1. (A) Section of normal testis of California gull at hatching. Seminiferous tubule (*ST*) contains PGC (arrows). Cortex (*C*) is squamous epithelium (×400). (B) California gull testis from egg injected with *o,p'*-DDT (2 ppm), showing cortical localization of PGC arrested in meiotic prophase (arrows) (×400; scale bar, 10 μm). (C) Reproductive organs of partially eviscerated male western gull hatchling injected during incubation with *o,p'*-DDT (5 ppm). Testes (*T*) are of normal shape. Feminization is indicated by the presence of left oviduct (double arrows), shell gland (*s*), and short right oviduct (single arrow). Other structures: mesonephros (*ms*), metanephros (*mt*), and cloaca (*cl*) (×3.5). (D) Reproductive organs of male western gull hatchling from egg injected with *p,p'*-DDT (10 ppm) and *p,p'*-DDE (40 ppm). Left gonad is enlarged and flattened into an ovotestis (*O*); left oviduct (double arrows) is present; right oviduct (single arrow) is prominent and edematous (×3.5; scale bar, 2 mm).

0036-8075/81/0821-0922$01.00/0